IMPACT DAMAGE ANALYSIS OF 3D WOVEN CARBON FIBRE COMPOSITES USING COMPUTED TOMOGRAPHY

E. Archer*, S. King, JP. Quinn, S. Buchanan, AT. McIlhagger
Engineering Composites Research Centre, University of Ulster, Jordanstown, Northern Ireland, BT37 0QB.
Corresponding author (e.archer@ulster.ac.uk)

1 Introduction

3D woven textile reinforced composites allow the optimisation and tailoring of specific material properties into the final component that can provide a reduction in manufacturing cost. This paper investigates the damage imparted to 3D orthogonal woven fabric composite by drop weight impact and compression after impact (CAI) testing. Furthermore, specimens are analysed using computed tomography (CT) and through transmission ultrasonic inspection to observe how an impact event affects the structural integrity of the 3D woven composite. The 3D multi-layer reinforcements were manufactured on a textile loom with few mechanical modifications to produce preforms with fibres orientated in the warp, weft and through-the-thickness (TTT) directions. Orthogonal structures represent one of the more straightforward structures in terms of tow path complexity, yet also provide a structure where the advantages of low crimp tows bound together by a binder tow, result in a composite with high performance and reduced sensitivity to interlaminar shear [1].

New commercial aircraft programmes such as the Airbus A350, Boeing 787 Dreamliner or Bombardier C-Series have increased the demand for polymer composite primary aircraft structures with a gradual move towards the use of liquid moulding resin transfer technology. This generally requires the use of a woven or stitched form of dry fabric rather than the more traditional methods of pre-impregnation of unidirectional tape. However, woven composites materials are susceptible to transverse impact loading which causes laminas to become delaminated [2]. Various methods have been developed to improve the impact tolerance including z-pinning, selective interlayers and hybrids, protective layers or resin toughening; one method that is becoming increasingly successful is to reinforce composites with a fibre that connects the layers together running from the upper to lower surface of the laminate. Mouritz et al. [3] stated that 3D woven composites have higher ballistic damage resistance and impact tolerance resistance than 2D materials, higher tensile strain and strain-to-failure values, and also higher interlaminar fracture toughness; this might be beneficial in the design of primary aircraft structures where the limiting design criteria is compression after impact. These TTT tows have been shown to provide not only increases in tensile [4], flexural strength and modulus of composite components, but also increases in the damage tolerance of a woven composite component [5].

Baucom and Zikry [6] have studied the effects of fibre reinforcement geometry on damage progression in woven composite panels under repeated drop-weight. In this study, 3D composites had the greatest resistance to penetration and dissipated more total energy than the other systems. Bahei-El Din looked at the impact damage of 3D woven composites penetrated by hemispherical projectiles [7], and 3D orthogonal hybrid woven composite under impact was studied by Lv [8]. It has been shown by Gama [9] that by having as little as 1-2% TTT reinforcement, delaminations are suppressed and interlaminar strength and fracture toughness is increased. Byun [10] also observed benefits in having TTT reinforcement in a reduction in damage area of between 30-40% compared to 2D composites.

With research showing increased mechanical properties of 3D woven composites in a number of areas, understanding of the failure of these advanced

composites is required. Through a comprehension of the failure mechanisms of these materials, design improvements can be implemented and the micro-structural features that degrade performance can potentially be eliminated, while those that enhance performance can be optimised [11].

Previous research on the failure of woven composites has shown that the CT technique affords several advantages over the conventional approach of parallel dissection followed by image analysis of polished surfaces, as it eliminates tedious sample preparation [12-14]. Besides the advantage of being non-destructive and non-invasive, CT allows a large amount of the internal geometry to be determined with a single scan, enabling internal cross-sections to be visualised, and in turn be reconstructed into three-dimensional volumes. Besides analysing internal structures and architectures, researchers have used CT to better understand the behaviour and damage of composite materials undergoing fatigue, tensile or impact loading [15–17]. The ability to detect and accurately measure features down to individual fibre breakages will aid future research; from the rigorous evaluation of damage models to understanding the fundamental physical mechanisms governing crack growth in composites.

2. Experimental

3D multi-layer woven reinforcements were designed using the X-Sectional design system to provide a representation of the structure, detailing the relative positions of the yarns and also generating the lifting plan to operate a Jacquard controlled loom (Figure 1). Fabrics were then manufactured on a conventional textile loom with mechanical modifications using Toray T300-12000 yarns (Table 1). The loom used was a DATAWEAVE loom with Jacquard controller incorporating 1152 hooks.

The approach adopted by the Engineering Composites Research Centre, University of Ulster denotes that the warp (or 0^o direction) tows are used to provide TTT binders that consolidate the preform. The TTT tows are arranged in different patterns and levels of the reinforcement according to the net shape and mechanical properties required for the final composite component. The textile preform design used in this study is a 3D representation of the 2D satin fabric structure. 2D satin weaves are very flat, have good wet out and a high degree of drape (the ability to form around a complex curvature). The low crimp gives good mechanical properties. Satin weaves allow tows to be woven in the closest proximity and can produce fabrics with a close ‘tight’ weave. The 3D representation of the satin fabric used for this work has seven layers of warp and six layers of weft. Three types of 3D woven fabrics were produced. All three were based on the satin harness structure with 5 weft stuffers below the float (shown in Figure 1) but with varied TTT binders, namely a 1x12k binder, a 2x6k binder and finally a 1x6k binder fabric.

Several woven composite plaques were manufactured using the VaRTM method. A caul plate was used in conjunction with a flexible membrane to consolidate the fabric reinforcements under full vacuum, prior to the injection of resin by peripheral gating at a tool temperature of 75 ^oC. Araldite LY564 and Hardener HY2954 (based on bisphenol A epoxy and a cycloaliphatic amine hardener) was mixed and degassed at 2.86:1 by weight before transfer of the resin. After injection, a ramp was applied up to 100^oC. The temperature was held isothermal for 60 minutes; the composite plaque was then de-moulded and post cured for a further 180 minutes at 140^oC. The composite specimens had a fibre volume fraction of approximately 46%

Impact testing was conducted as required by SACMA SRM 2R-94 test standard [18]. Thirty samples in total were tested, which equated to ten per composite (five impacted on the binder middle and five on the binder edge (Fig. 1)). Impact depth data for the three composites (1x12k, 2x6k, and 1x6k) used within this research is shown in Table 2.

Initially optical microscopy was used to observe the undamaged composite structure and then Computed tomography (CT) was used to observed damage after impact. X-ray images at different angular views were used to calculate a three-dimensional volumetric model of the object. The volume data was then analysed to find the position and size of defects and cracks after impact. The CT scan was conduced using a Phoenix v|tome|x s from GE equipped with a Perkin Elmer flat panel (512x512 px, 400 µm pix size). The X-ray tube was operated

at 150 kV and 230 µA. The Voxel resolution was 41 µm.

After impact, samples were strain gauged and secured within the CAI testing rig. The CAI rig is described within the SACMA SRM 2R-94 test standard and is based on the Boeing Model No. CU-CI CAI testing rig. The rig has anti buckling rails on either side of the vertical supports to ensure than the sample does not slip during testing.

3. Results

Table 2 shows that impact depth for samples impacted at the binder edges were deeper by up to 0.89mm than those impacted in the middle of the binder which equates to a difference of up to 97%. This suggests a relationship exists between impact location and impact depth. By observing the CT scans and micrographs it was determined that the difference in depth is due to the energy absorption mechanisms within each area i.e. within the binder edge impacts this is matrix shearing and tensile rupture, and within the binder middle impact area the main energy absorption is via delaminations. Measurements made of the visual impact damage were observed to be greater in the warp direction than in the weft on both the impact and non-impact surfaces. It was also observed that the damage area on the non-impact surface was greater than that on the impact surface confirming that damage spreads TTT in a cone effect (Figures 5 and 7).

Compression after impact results (Table 3) showed that CAI strength values (when %CV values are considered) with respect to impact locations were roughly the same, implying that unlike impact depth, there was no relationship found to exist between CAI strength and impact location. CAI strength was greatest within the 2x6k composites with the 1x6k having similar values and the 1x12k the lowest.
The results indicate that the 2x6k binder composites have the highest CAI strength for both binder middle and binder edge impacted samples, followed by the 1x6k binder composites and lastly the 1x12k binder composites. When CAI values are considered with respect to impact location it can be concluded that although impact location has been observed to be related to impact depth it has no influence on the CAI strength. On observation of micrographs it was noted that the 2x6k binder fabric had the smallest percentage crimp within the warp tows, which are the main load bearing fibres during compression. This reduction in crimp has been observed to be very influential in tensile, flexural and ILSS properties in previous studies also [1]. The CAI values for these woven fabrics which varied between 131MPa and 141MPa were lower than values previously reported by Brandt et al. [19] of over 200MPa. However, recently University of Ulster have been developing new orthogonal low crimp 3D woven architectures using HTA/HTS fibres [20-21] which have been found to give a CAI value of up to 220MPa, and 5D woven structures that also have a CAI value of 220MPa (6.7J/mm) [23].

The CT scans (Figure 2-5) shows the influence the binders have on the surrounding stuffers. Stuffers can become crimped locally or misaligned due to the binders pinching the stuffers as they go TTT. The micrograph of the undamaged composite (Figure 6) shows how the weft stuffers can be pulled into the resin rich area between the warp stuffer stacks due to the binder going through-the-thickness. As the weft stuffers are pulled they pinch the edges of the warp stuffer tows distorting their shape and misaligning the warp stuffer stack itself. It was found that using binders with different tex values influence the size of the resin rich area which is created as the binders go through-the-thickness.

Figure 6 shows the crack following the TTT binder. It shows that while a large amount of damage has occurred around the area of fracture, the binder has not ruptured and this impedes the spread of delaminations from the impact site; the amount of spread of delamination damage is therefore reduced.

4. Conclusion

-Impact depth for samples impacted at the binder edges were deeper than those impacted in the middle of the binder.
-2x6k binder composites have the highest CAI strength followed by the 1x6k binder composites and lastly the 1x12k binder composites.
-CT was used to observe extent of internal impact damage.

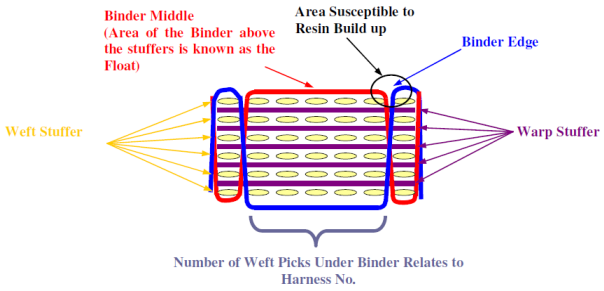

Figure 1. Orthogonal Woven Structure.

Table 1. Details of fibres used.

Fibre Manufacturer	Toray Industries	
Fibre Name/Designation	T300-6000 (6k)	T300-12000 (12k)
Number of Filaments	6000	12000
UTS (MPa)	3530	3530
Tensile Modulus (GPa)	230	230
Elongation (%)	1.5	1.5
Mass per Unit Length tex (g/1000m)	396	800
Density (kg/m^3)	1760	1760

Table 2. Details of impact testing.

	1x12k			2x6k			1x6k		
Specimen	Sample Thickness (mm)	Impact Energy (J)	Impact Depth (mm)	Sample Thickness (mm)	Impact Energy (J)	Impact Depth (mm)	Sample Thickness (mm)	Impact Energy (J)	Impact Depth (mm)
Binder Middle Impact									
Average	3.10	20.77	0.91	3.16	21.074	0.97	2.80	18.73	1.63
St Dev	0.12	0.82	0.24	0.03	0.24	0.24	0.019	0.11	0.55
% CV	3.93	3.94	26.5	0.96	1.13	24.93	0.66	0.56	33.57
Binder Edge Impact									
Average	3.20	21.46	1.8	3.15	21.094	1.64	2.81	18.85	2.18
St Dev	0.09	0.62	0.7	0.03	0.18	0.22	0.046	0.32	0.61
% CV	2.81	2.87	38.95	0.96	0.87	13.58	1.63	1.71	27.78

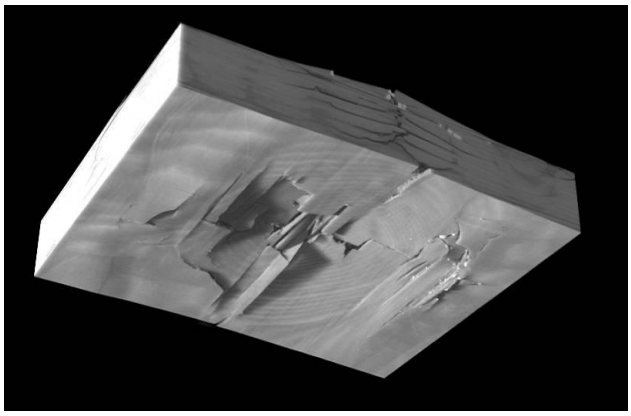

Fig.2. Three-dimensional volumetric model showing impact surface.

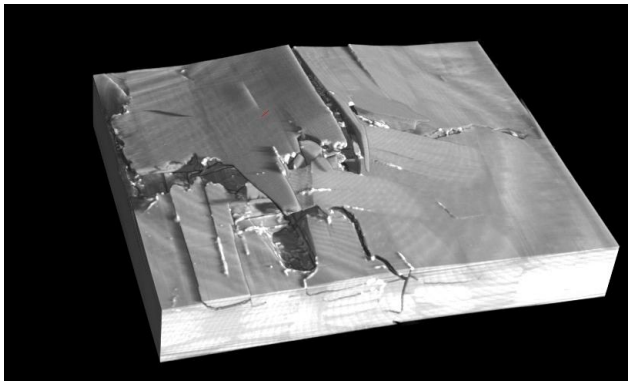

Fig.3. Three-dimensional volumetric model showing non-impact surface.

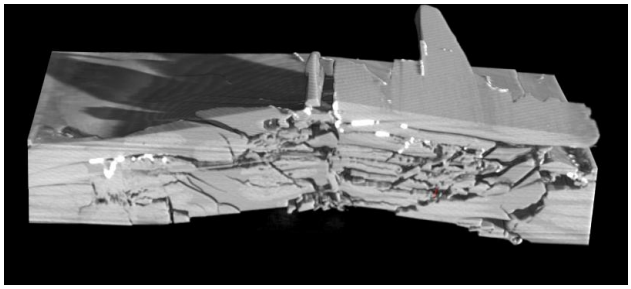

Fig 4. Three-dimensional volumetric model showing cross section at the centre of the impact.

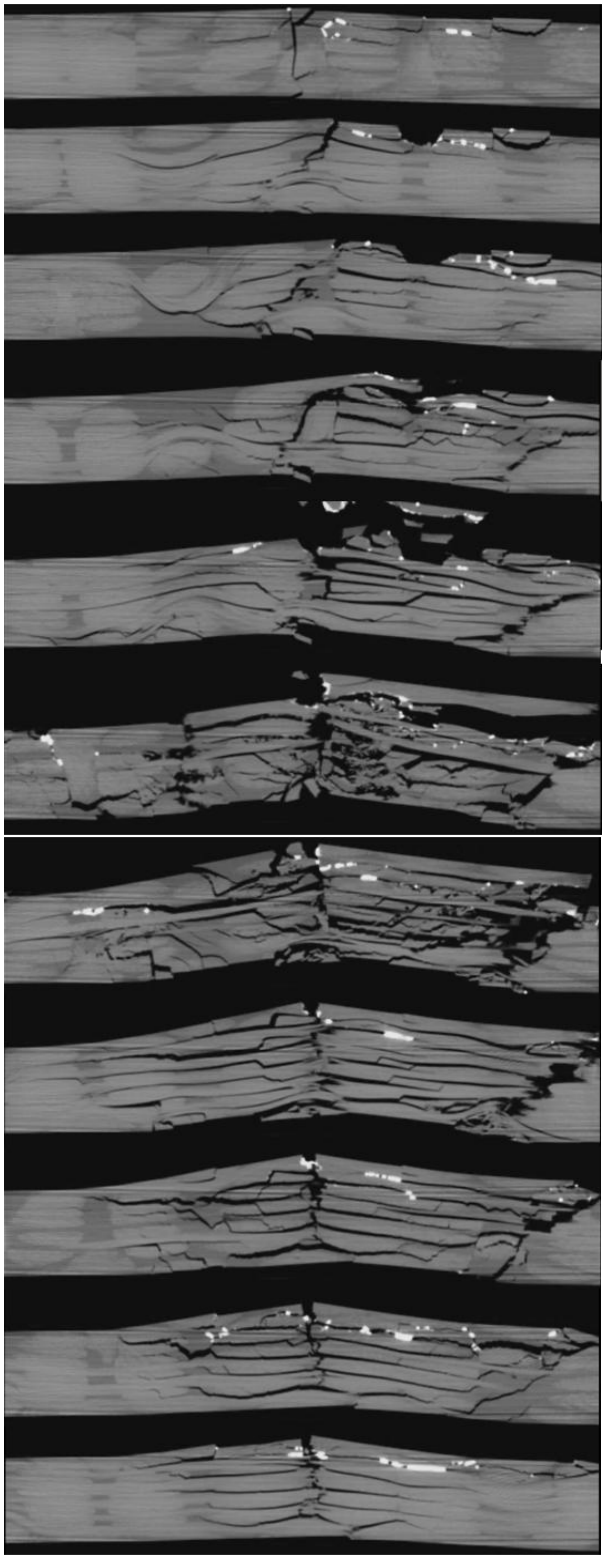

Figure 5. Slices taken using CT scan in weft direction- 1x12k binder after impact.

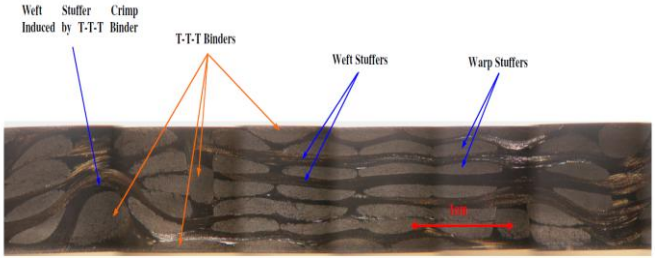

Fig 6. Undamaged composite structure 1x12k binder, weft direction.

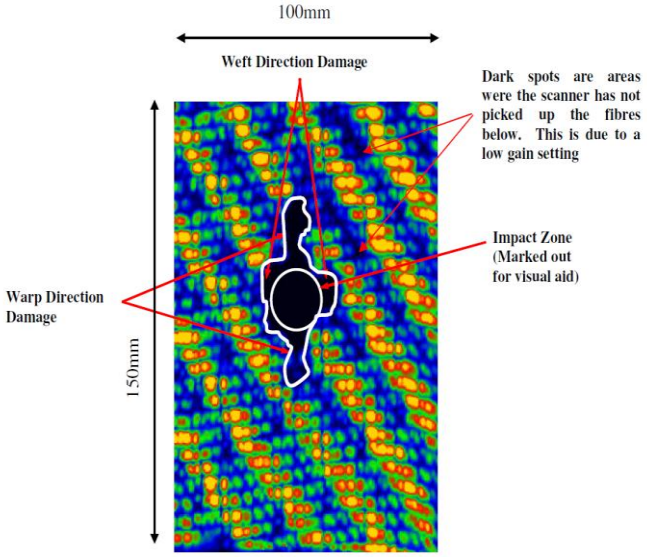

Figure 7. C-Scan of impacted specimen.

Table 3. Details of CAI strength.

	1x12k Binders		2x6k Binders		1x6k Binders	
Specimen	Compression Load (kN)	CAI Strength (MPa)	Compression Load (kN)	CAI Strength (MPa)	Compression Load (kN)	CAI Strength (MPa)
Binder Middle Impact						
Average	40.5	131.1	44.7	141.4	37.9	135.6
St Dev	2.1	8.6	2.04	5.8	0.33	11.2
% CV	5.3	6.55	4.56	4.14	8.89	8.3
Binder Edge Impact						
Average	41.4	129.3	45.2	143.7	36.2	134.4
St Dev	1.4	4.1	1.7	5.6	2.5	7.7
% CV	3.43	3.15	3.74	3.87	6.99	5.74

5. References

[1] King RS., Stewart G., McIlhagger AT., Quinn JP., 'The influence of through the thickness binder yarn count on fibre volume fraction, crimp and damage tolerance within 3D woven carbon fibre composites,' Polymers and Polymer Composites, 17(5), 303 (2009).

[2] Atas, C., Liu, D., 'Impact Response of woven composites with small weaving angles,' Int. J. Impact Eng., 35 (2), 80 (2008).

[3] Mouritz, A.P., Bannister, M.K., Falzon, P.J., Leong, K.H., 'Review of applications for advanced three-dimensional fibre textile composites', Composites Part A., 30 (12), 1445 (1998).

[4] Cox BN, Dadkhah MS., and Morris WL., 'On the Tensile failure of 3D woven composites,' Composites Part A., 27, 447 (1996).

[5] Cox BN., Dadkhah MS., Morris WL., and Flintoff JG., 'Failure Mechanisms of 3D Woven Composites in Tension, Compression, and Bending,' Acta Metall. Mater., 42 (12), 3967 (1994).

[6]. Baucom, JN. and Zikry, MA., 'Low-Velocity Impact Damage Progression in Woven E-Glass Composite Systems,' Composites Part A., 36, 658 (2005).

[7] Bahei-El-Din, YA., Zikry, MA., and Rajendran, AM., **'**Impact-induced deformation fields in 3D cellular woven composites,' Compos. A., 34(8), 765 (2003).

[8] Lv, L., Sun, B., Qiu,Y., and Gu, B.**, '**Energy absorptions and failure modes of 3D orthogonal hybrid woven composite struck by flat-ended rod,' Polymer Compos., 27(4), 410 (2006).

[9] Gama, BA., Harque Md.J., and Gillespie, JW., Bogdanovich, AE., 'Impact, damage, and energy absorption of a 3D orthogonal weave composite unit cell model,' 49th International SAMPE Symposium, Long Beach, CA May 16, (2004).

[10] Byun, J-H., Song, S-W., Lee, C-H., Um, M-K., and Hwang, B-S., 'Impact properties of laminated composites with stitching fibres,' Composite Structures, 76 (1-2), 21 (2006).

[11] Chou, S., Chen, H., Chen, H., 'Effect of weave structure on mechanical fracture behaviour of three dimensional carbon fibre fabric reinforced epoxy resin composites,' Compos Sci Technol., 45, 23 (1992).

[12] Desplentere, F., Lomov SV., Woerdeman DL., Verpoest, I., Wevers, M., Bogdanovich, A., 'Micro-CT characterization of variability in 3D textile architecture,' Compos Sci Technol., 65, 1920 (2005).

[13] Djukic, LP., Herszberg, I., Walsh, WR., Schoeppner, GA., Prusty, BG., Kelly, DW., 'Contrast enhancement in visualisation of woven composite tow architecture using a micro CT scanner. Part 1: fabric coating and resin additives,' Compos Part A., 40, 553 (2009).

[14] Djukic, LP., Herszberg, I., Walsh, WR., Schoeppner, GA., Prusty, BG., 'Contrast enhancement in visualisation of woven composite architecture using a micro CT scanner. Part 2: tow and preform coatings,' Compos Part A., 40, 1870 (2009).

15] Xiao Y, Ishikawa T., 'Bearing strength and failure behaviour of bolted composite joints (part I: experimental investigation),' Compos Sci Technol., 65, 1022 (2005).

[16] Tan, KT., Watanabe, N., Iwahori, Y., 'X-ray radiography and micro-computed tomography examination of damage characteristics in stitched composites subjected to impact loading,' Composites: Part B., 42, 874 (2011).

[17] Schilling, PJ., Karedla, BPR., Tatiparthi, AK., Verges, MA., Herrington PD., 'X-ray computed microtomography of internal damage in fiber reinforced polymer matrix composites,' Compos Sci Technol., 65, 207 (2005).

[18] SACMA Recommended Method SRM 2R-94, 'Compression After Impact Properties of Oriented Fiber-Resin Composites," Suppliers of Advanced Composite Materials Association, Arlington, Virginia, 1994.

[19] Brandt, J., Drechslef, K., & Arendtsb, F-J., 'Mechanical performance of composites based on various three-dimensional woven-fibre preforms,' Composites Science and Technology, 56, 381 (1996).

[20] Archer, E., Buchanan, S., McIlhagger, AT., Quinn. JP., Morgan, M., 'An investigation on the effect of 3D weaving on carbon fibre tows, fabrics and composites,' Proceedings of the 9th International Conference on Textile Composites (Texcomp9), 371 (2008).

[21] Buchanan, S., Grigorash, A., Archer, E., McIlhagger, AT., Quinn, JP., Stewart, G., 'Analytical Elastic Stiffness Model for 3D Woven Orthogonal Interlock Composites,' Composite Science and Technology, 70(11), 1597 (2010).

[23] McIlhagger, R., Quinn, JP., McIlhagger, AT., Wilson, S., Simpson, D., Wenger, W., 'The influence of binder tow density on the mechanical properties of spatially reinforced composites. Part 1 – Impact resistance,' Composites Part A., 38 (3), 795 (2007).